

Reconstruction of the Annual Variation in Solar Radio Flux and the Catania Sunspot Area from Tree Ring-index Time Series

J. O. Murphy, H. Sampson

Department of Mathematics, Monash University,
Clayton, Vic. 3168

T. T. Veblen, R. Villalba

Department of Geography, University of Colorado,
Boulder, CO 80309, USA

Abstract: Four tree ring-index site chronologies, representing standardised annual growth rates for spruce trees growing at high altitude sites in Colorado, have been employed as proxy data in a regression model for the annual variation of solar radio flux at 2800 MHz ($F_{10.7}$) and the Catania sunspot area (A_C). These dendrochronological time series all exhibit significant power spectrum peaks at about 11 years and separately correlate with the annual values of R_Z , $F_{10.7}$ and A_C , as solar activity indicators. The two models constructed give the cyclic variation of $F_{10.7}$ and A_C back to AD1673.

1. Introduction

There are several distinct indicators, established by ground-based observations or satellite instrumentation, which convey the level of solar activity over the 11-year cycle. In addition to the Zürich relative sunspot numbers R_Z , some other measures are given by the variation of solar radio flux at 2800 MHz $F_{10.7}$, the Catania sunspot area A_C , the polar magnetic field strength, number of polar faculae, coronal hole size and geomagnetic indices. Most of these records only extend over the equivalent length of a few solar cycles, in contrast to the near three-century compilation of annual sunspot numbers. Not all of these records cross-correlate significantly. Generally the $F_{10.7}$ and A_C data are considered to be more accurate quantifiers than R_Z values which, apart from observational difficulties, are also subject to an observer correction factor. However, when considered as annual averages, the longer time series for activity indicators (i.e. R_Z , $F_{10.7}$, A_C , aa) exhibit significant power spectrum peaks around 11 years and demonstrate a high level of cross-correlation. Linear regression equations for monthly R_Z , based on smoothed monthly values of these and other indicators, have been given by Layden *et al.* (1991). They employed these relationships when considering methods for forecasting maximum activity epochs. In this work we are restricted to

using annual averages, as the model for R_Z is based on annual proxy tree-ring index data. Together with tree-ring time series, other series obtained from ice cores and sedimentary layers can also provide proxy data on cyclic solar-terrestrial interactions (Castagnoli *et al.* 1991; Ghil 1991).

Overall, our objective is to model past annual variations in $F_{10.7}$ and A_C based on a tree-ring index model for R_Z , utilising the high level of correlation that exists between R_Z and these indicators. A comparison of the waveforms, over the period of recorded values, will give an indication of amplitude and phase concurrence. It should be possible to model these indicators over the Maunder minimum epoch and earlier downturns in solar activity, provided longer tree-ring records, which correlate significantly over the period of the existing sunspot record, can be established.

2. Data

The data sets employed fall into two groups—the solar activity indicators R_Z , $F_{10.7}$, A_C and the proxy data given by tree ring-index time series which exhibit a dominant near-11-year spectral periodicity. The $F_{10.7}$ radio flux data extend from AD1949 to 1988, and those for the sunspot area A_C , given in fractional units of millionths of a solar disk, from AD1958 to 1985. The distribution of the monthly values for these two indicators is given over about three solar cycles in Figure 1.

After smoothing, the $F_{10.7}$ signal profile shows that well-defined levels of near-maximum activity extend over about 3–4 years. Each cycle is characterised by a rapid rise to maximum activity, similar to R_Z variation for high-activity cycles, followed by a two-stage decline to minimum activity. The first stage of rapid decline is followed by a second stage of gradual decline over about the last four years of the cycle.

A scatter plot showing the distribution of $F_{10.7}$ and R_Z annual values is given in Figure 2a together with the regression line

$$F_{10.7} = 57.902 + 0.887 R_Z, \quad (1)$$

which essentially represents the longer-term average annual relationship between these two indicators. The positive constant in this linear expression indicates that in the absence of sunspots there is still some residual radio flux. The regression model explains over 95% of the variance. Figure 2b gives the equivalent relationship between A_C and R_Z with

$$A_C = 11.353 R_Z + 0.0373 R_Z^2. \quad (2)$$

In this case a quadratic relationship has been introduced to relate sunspot area and number; no constant term was included in the regression with

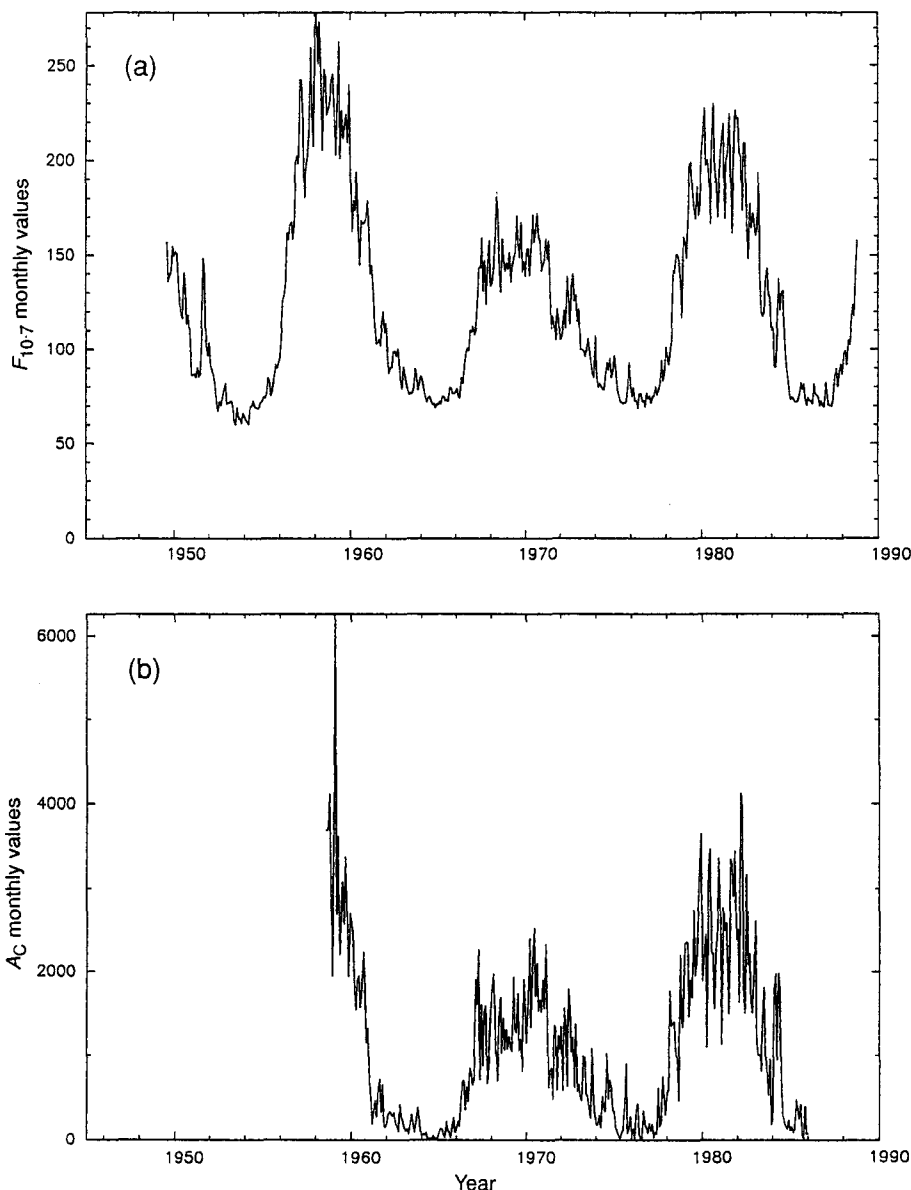


Figure 1—Monthly variation in (a) $F_{10.7}$ radio flux and (b) A_C sunspot area.

the expectation that $A_C = 0$ when $R_Z = 0$. The percentage variance explained is again near 95%.

A model for R_Z annual variation has been based on four high altitude spruce [*Picea engelmannii* (Parry) Engelm.] tree-ring index site chronologies from Colorado, which extend over the common interval from AD1673 to 1986. Two sites (CSA, CSB) are located on opposite sides of the Cache La Poudre River (Veblen *et al.* 1991a) and one at Long Lake (LL3), in northwestern Rocky Mountain Park, and the fourth in the Ripple Creek Pass area (RC), White River National Forest (Veblen *et al.* 1991b). This model is an extension of the one described by Murphy *et al.* (1993), in which only two tree ring-index chronologies from the Cache La Poudre River area were used. The addition of two more proxy data sets has contributed to

improved signal continuity. Again, the choice of these additional tree-ring chronologies was based on the existence of a dominant near-11-year spectral signal and a high level of cross-correlation and cross-spectral amplitude with the R_Z time series. The identification of these further chronologies from sites over a wide geographical region also diminishes the probability that the 11-year signal is just a random growth response at a single site.

While the 11-year signal is the common feature associated with the four chronologies, it is only one component of each frequency spectrum, which also contains growth responses to both local and regional influences and site disturbances that are of a temporal nature, as well as noise. These other signals may not be common to all the chronologies considered; hence, it was necessary to

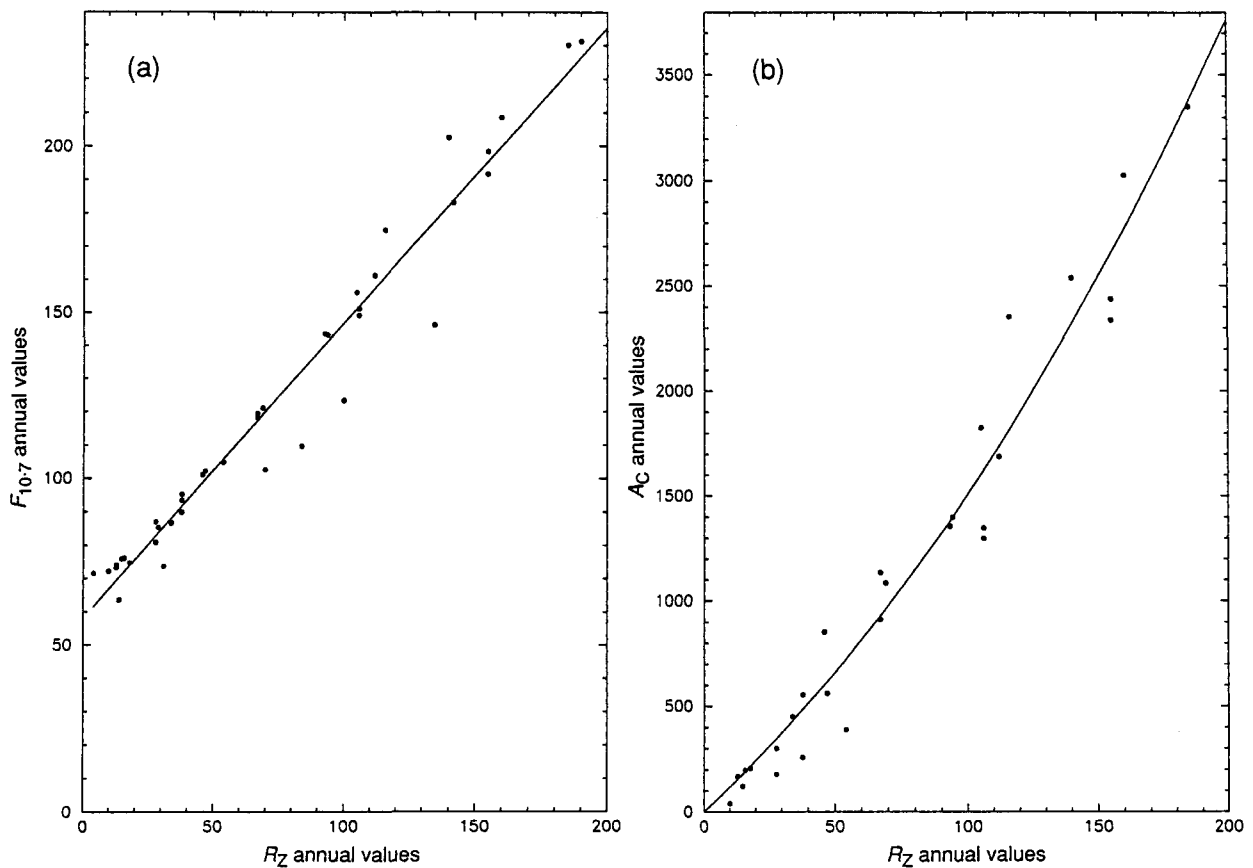


Figure 2—Scatter plot and regression line for annual values of R_Z and (a) $F_{10.7}$ values for radio flux (see equation 1) and (b) A_C values for sunspot area (see equation 2).

apply three different combinations of notch, high- and low-frequency digital filters to resolve the 11-year signal in each time series.

Table 1. Filters used for signal resolution

The values given for low- and high-pass filters correspond to their 50% frequency response cutoff and those for the notch filters correspond to the central frequency

Chronology	Filter		
	Low (yr)	High (yr)	Notch (yr)
CSA	5	30	4, 16
CSB	5	30	4, 16
LL3	5	30	4, 16
RC	5	30	4, 15, 22

These filters were applied to each chronology in a sequential manner and at each stage the spectral profile of the filtered series was generated. The nature of this profile determined the next appropriate filter type, which was generated by the statistical software package BMDP (Dixon *et al.* 1985). In conjunction, the frequency response function of each filter applied to a particular time series was plotted to determine the percentage of signal at each frequency passed or rejected. The initial objective of the filtering procedure was to reduce long-term variance greater than thirty years and short-term variance less than five years. Notch filters were

then applied to reduce the variance associated with any dominant spectral peaks, on either side of the frequency of interest, which may contribute unwanted influence in the reconstruction model. The notch filter bandwidths were kept as narrow as possible so only those frequencies targeted were affected. This approach ensures that most of the variance about the frequency of 0.09 cycles per year is retained in an endeavour to match the spectral profile of the R_Z time series. The nature of the filters employed is contained in Table 1 and, as an example, the frequency response functions for the filters applied to the CSA chronology are given in Figure 3. From the table it can be noted that the same filtering sequence was applied for both the CSA and CSB sites, which are nearby.

3. Results and Discussion

From the regression model, annual values of R_Z for year t are given by a linear combination of $I_i(t)$, the ring index values from the filtered series, with the index i designating the site chronology. The model variation of radio flux at year t , in terms of the proxy data, is given by

$$F_{10.7}(t) = 83.000 + 0.253 a_0 + 0.514 \sum_{i=1}^4 a_i I_i(t) - 0.261 \sum_{i=1}^4 b_i I_i(t+1).$$

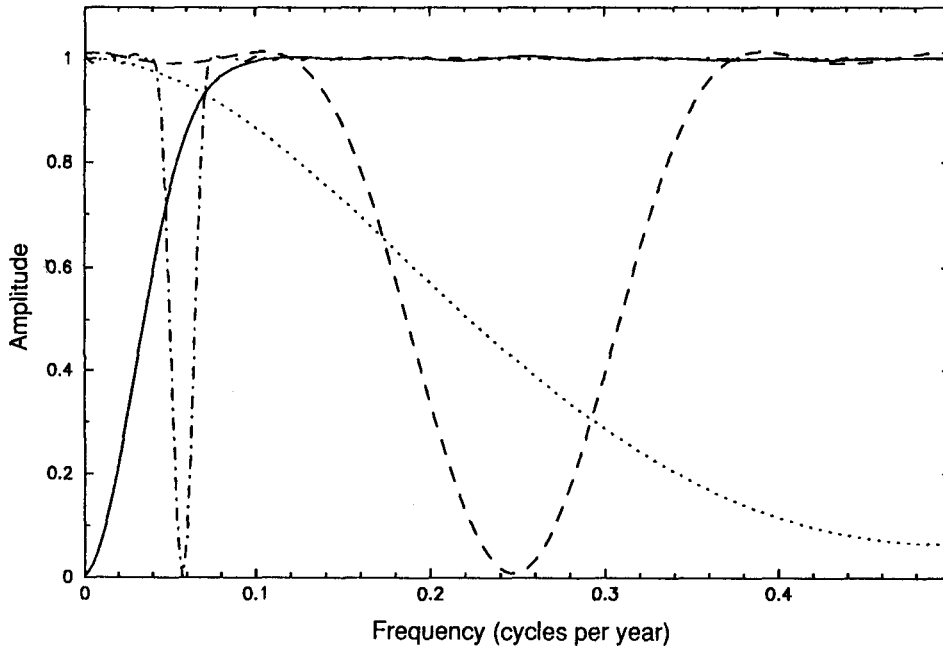


Figure 3—Plot of frequency response functions derived for the four filters applied to the Colorado spruce site A chronology: 30-year high-pass filter (full curve), 5-year low-pass filter (dotted curve), 16-year notch filter (dot-dash curve) and 4-year notch filter (dashed curve).

This expression follows from regression over the annual values for $F_{10.7}$ variation and also accounts for the persistence (i.e. autocorrelation) in tree growth in the following year by inclusion of the terms at year $(t+1)$. All the regression coefficients are significant at $P < 0.05$.

In a similar way the Catania sunspot area at year t is given by

$$A_C(t) = 4.270 a_0 + 5.990 \sum_{i=1}^4 a_i(t) I_i(t) + 1.720 \sum_{i=1}^4 b_i I_i(t+1) + 0.001 \left(c_0 + \sum_{i=1}^4 c_i I_i(t) \right)^2 - 0.005 \left(d_0 + \sum_{i=1}^4 d_i I_i(t+1) \right)^2$$

Smoothed model values for $F_{10.7}$ and A_C , over AD1673 to 1986, are shown in Figures 4a and 4b along with the smoothed recorded values over approximately three solar cycles to 1986. Clearly there is consistency in phase, which is established by the nature of the corresponding lagged cross-correlation functions with maximum value at lag 0, as shown in Figure 5. There is good model replication of A_C values over the entire 11-year cycle, while the $F_{10.7}$ model values do not match as well over the high and low cycle values. This outcome

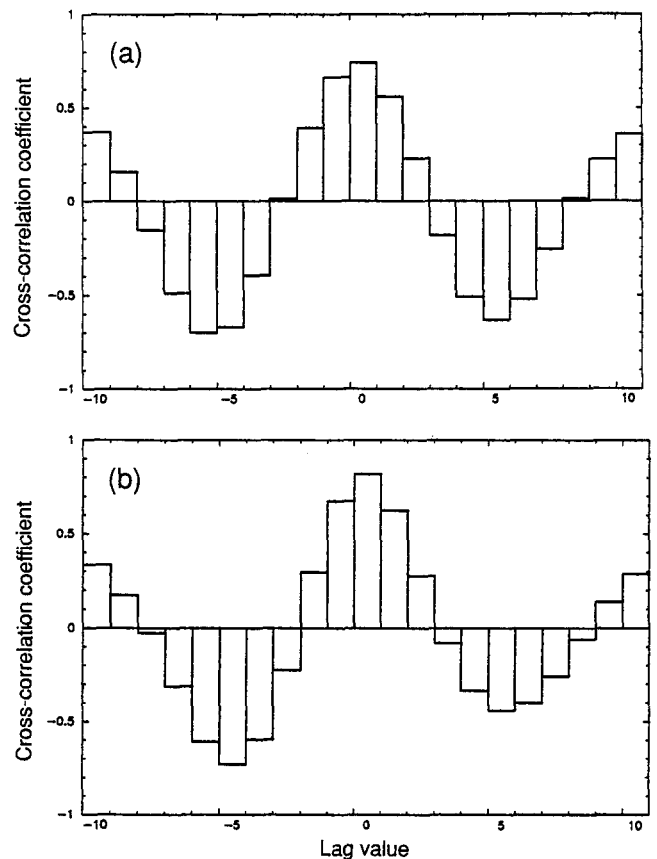


Figure 5—Lagged cross-correlation functions for the model and actual data for (a) $F_{10.7}$ and (b) A_C . They are characteristic of periodic functions, indicate the level of correlation, and have maximum value at lag 0, which establishes phase correspondence.

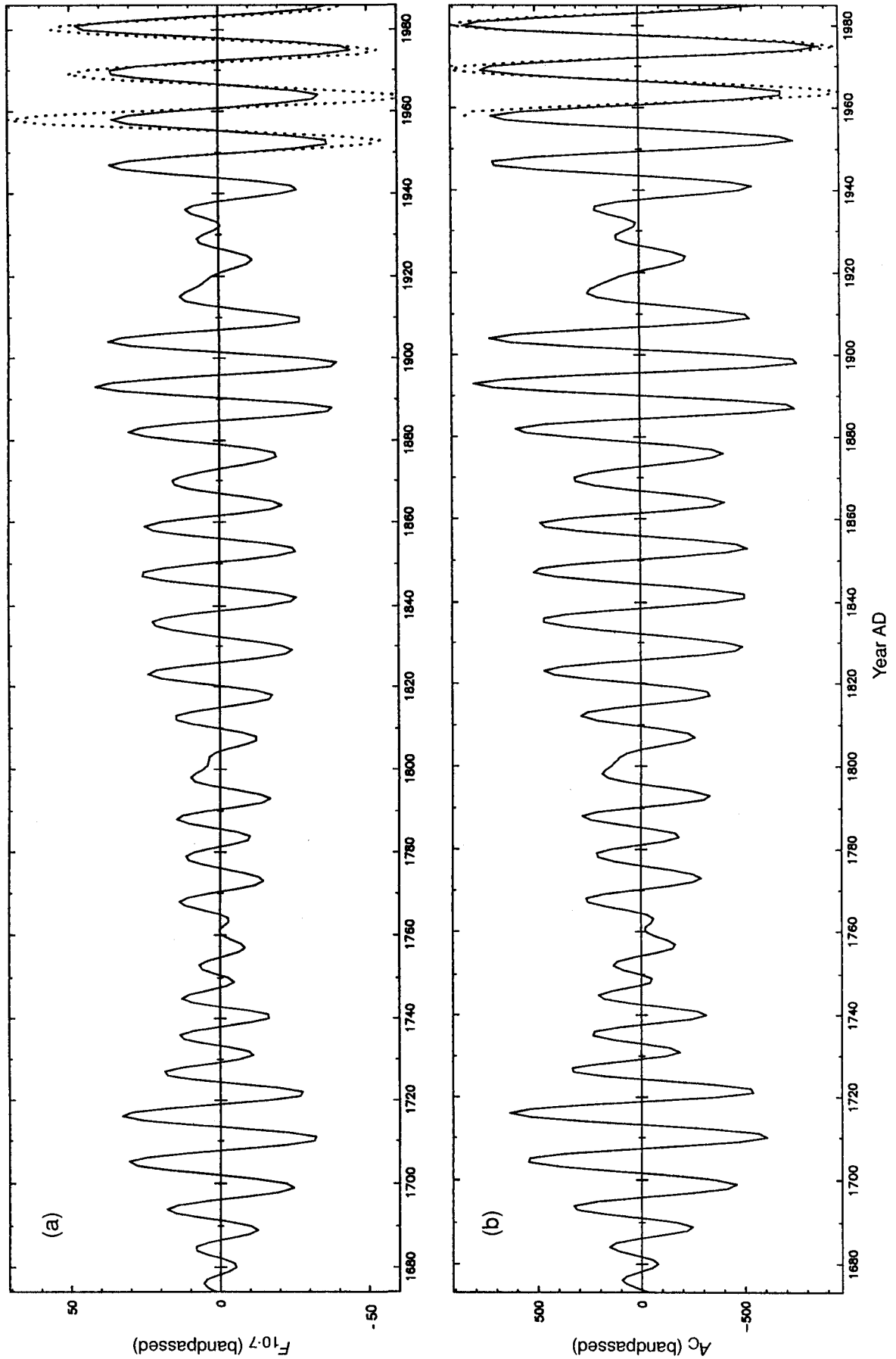


Figure 4—Smoothed model values (full curves) and actual data values (dashed curves) for (a) $F_{10.7}$ radio flux and (b) A_c sunspot area.

is not uncharacteristic of any regression process which minimises the sum of the squares of the residuals. However, on comparison it would appear that these tree growth patterns, with significant spectral variance near 11 years, are a reasonable proxy for the annual variation in sunspot area as defined by A_C values. The correlation values over the common year range are $r = 0.74$ for $F_{10.7}$ (at the 99% confidence level $r = 0.42$) and $r = 0.82$ for A_C ($r = 0.49$). As the variation in solar ultraviolet radiation closely parallels the $F_{10.7}$ variation, it could be expected that Figure 4a also gives the scaled cyclic form of solar UV variability. The modelled variations show considerable amplitude modulation in the 11-year periodicity over three centuries, with an indication of a Gleissberg period of about eight solar cycles. The recent levels of high solar activity are replicated in each case. Over the years AD1920 to about 1940 there is a loss of coherent signal and likewise for a short time around AD1760.

This procedure can be extended to model other solar cycle indicators based on their regression relationship with R_Z . Alternatively it is possible to establish a direct relationship between the activity indicator and the proxy tree-ring data. However, it was considered preferable to utilise the long baseline of R_Z values together with the essentially noisy tree-ring data to arrive at the best model. The calibration (regression) and verification phases otherwise would be based on only about 1.5 cycles, which is hardly adequate to explain a large percentage of the variance

or replicate the cyclic structure. Unfortunately, the models have no predictive value for forecasting the level of future solar activity. Periodic extrapolation has not been very successful in past forecasts.

Finally, we are not inferring that variations in $F_{10.7}$ radio flux will directly influence tree growth. However, at these high altitude sites, changes in UV levels which, in percentage terms, are a lot higher than changes in total irradiance over the solar cycle, could have some direct influence. The most likely solar-terrestrial connection is via climate; any linkage remains to be established.

- Castagnoli, G. C., Bonino, G., Provenzale, A., 1991, In *The Sun in Time*, C. P. Sonett *et al.* (eds), University of Arizona Press, p. 562.
- Dixon, W. J. (chief editor), Brown, M. B., Engelman, L., Frane, J. W., Hill, M. A., Jennrich, R. I. and Toporek, J. D., 1985, *BMDP Statistical Software*, University of California Press.
- Ghil, M., 1991, In *The Sun in Time*, C. P. Sonett *et al.* (eds), University of Arizona Press, p. 511.
- Layden, A. C., Fox, P. A., Howard, J. M., Sarajedini, A., Schatten, K. H. and Sofia, S., 1991, *Sol. Phys.*, **132**, 1.
- Murphy, J. O., Veblen, T. T. and Sampson, H., 1993, *Proc. Astron. Soc. Aust.*, **10**, 196.
- Veblen, T. T., Hadley, K. S. and Reid, S., 1991a, *J. Biogeog.*, **18**, 707.
- Veblen, T. T., Hadley, K. S., Reid, M. S. and Rebertus, A. J., 1991b, *Can. J. For. Res.*, **21**, 242.

Manuscript received 14 September 1993,
accepted 26 April 1994